

# Synthesis and Optical Properties of Thiol-Stabilized PbS Nanocrystals

Xusheng Zhao,<sup>†,‡</sup> Ivan Gorelikov,<sup>‡</sup> Sergei Musikhin,<sup>§</sup> Sam Cauchi,<sup>§</sup>  
Vlad Sukhovatkin,<sup>§</sup> Edward H. Sargent,<sup>§</sup> and Eugenia Kumacheva<sup>\*,‡</sup>

Guangzhou Institute of Chemistry, Chinese Academy of Science, P.O. Box 1122,  
Guangzhou 510650, People's Republic of China, and Department of Chemistry, University of  
Toronto, 80 Saint George Street, Toronto, Ontario, Canada M5S 3H6, and Department of  
Electrical and Computer Engineering, University of Toronto, 10 King's College Road,  
Toronto, Ontario, Canada M5S 3G4

Received May 21, 2004. In Final Form: November 8, 2004

Thiol-capped water-soluble PbS nanocrystals (NCs) stabilized with 1-thioglycerol, dithioglycerol, or a mixture of 1-thioglycerol/dithioglycerol (TGL/DTG) were prepared via one-stage synthesis at room temperature. We found that NCs stabilized with a TGL/DTG mixture show efficient and stable infrared photoluminescence centered in the second "biological window" (1050–1200 nm). Under optimized conditions, full width at half-maximum of the PL emission peak was from 70 to 100 nm. PbS NCs were stable to precipitation and aggregation for the time period from 2 to 3 months when stored in the dark under room temperature. Room-temperature photoluminescence quantum efficiency of NCs was from 7 to 10%. When NCs were stored at 37 °C, their PL emission red-shifted, consistent with the NC growth.

## Introduction

Over the past decade, semiconductor nanocrystal quantum dots have attracted interest due to their size-tunable optical properties arising from the effect of quantum confinement.<sup>1–8</sup> In optoelectronics, size tunability of quantum dots allows control over the spectral range of absorption, photoluminescence, stimulated emission, and electroluminescence spectra,<sup>9–12</sup> whereas, in biological applications, this allows spectral multiplexing and coding.<sup>13</sup> In both areas of applications, photoluminescence in the near-infrared spectral range is of great demand: in optoelectronics to bridge interconnects with short- and medium-haul networks, and in biological applications to

exploit the transparent window in spectrum of absorption by water and biological materials such as oxy- and deoxyhemoglobin.<sup>14</sup>

The bulk-phase PbS has a band gap energy of 0.41 eV (at 300 K). Since this gap is larger than in other lead chalcogenides, such as PbSe and PbTe, it is not necessary to synthesize ultrasmall PbS nanocrystals to adjust the effective gap across the 1000–1500 nm spectral region. Recent progress in the use of PbS NCs includes their electroluminescence in a polymer matrix,<sup>15</sup> room-temperature optical gain in a glass matrix,<sup>16</sup> and, most recently, room-temperature optical gain in solution-processed PbS NC films.<sup>17</sup> In addition, PbS quantum dots are expected to have promising third-order nonlinear optical properties.

Previous aqueous-based syntheses of PbS nanoparticles employed water-soluble polymer stabilizers: poly(vinyl alcohol), poly(vinyl pyrrolidone), gelatin, and DNA.<sup>18,19</sup> These synthetic routes, however, did not produce PbS NCs with good optical properties, such as absorption or luminescent emission. More recently, PbS NCs with tunable size and good optical properties have been obtained by an organometallic method,<sup>20</sup> the drawback of this approach however was the use of organic solvents and high-temperature reaction conditions.

Recently, our group reported a route to the synthesis of water-soluble PbS nanoparticles stabilized with a mixture of thiols (1-thioglycerol and dithioglycerol).<sup>21</sup> The NCs combined features so far demonstrated in isolation:

<sup>†</sup> Chinese Academy of Science.

<sup>‡</sup> Department of Chemistry, University of Toronto.

<sup>§</sup> Department of Electrical and Computer Engineering, University of Toronto.

(1) Murray, C. B.; Norris, D. J.; Bawendi, M. G. *J. Am. Chem. Soc.* **1993**, *115*, 8706.

(2) (a) Alivisatos, A. P. *Science* **1996**, *271*, 933. (b) Bruchez, M.; Moronne, M.; Gin, P.; Weiss, S.; Alivisatos, A. P. *Science* **1998**, *281*, 2013.

(3) Li, J. J.; Wang, Y. A.; Guo, W.; Keay, J. C.; Mishima, T. D.; Johnson, M. B.; Peng, X. *J. Am. Chem. Soc.* **2003**, *125*, 12567.

(4) Chan, W. C. W.; Nie, S. M. *Science* **1998**, *281*, 2016.

(5) Redl, F. X.; Cho, K.-S.; Murray, C. B.; O'Brien, S. *Nature* **2003**, *423*, 968.

(6) Rogach, A. L.; Kornowski, A.; Gao, M.; Eychmuller, A.; Weller, H. *J. Phys. Chem. B* **1999**, *103*, 3065.

(7) Liang, Z.; Susha, A.; Caruso, F. *Chem. Mater.* **2003**, *15*, 3176.

(8) (a) Zhang, J.; Coombs, Neil.; Lin, Y.; Sargent, E. H.; Kumacheva, E. *Adv. Mater.* **2002**, *14*, 1756. (b) Lin, Y.; Zhang, J.; Sargent, E. H.; Kumacheva, E. *J. Mater. Sci.* **2004**, *39*, 993.

(9) (a) Huynh, W. U.; Dittmer, J. J.; Alivisatos, A. P. *Science* **2002**, *295*, 2425. (b) Klimov, V. I.; Mikhailovsky, A. A.; Xu, Su; Malko, A.; Hollingsworth, J. A.; Leatherdale, C. A.; Eisler, H.-J.; Bawendi, M. G. *Science* **2000**, *290*, 314.

(10) Zeng, Z. H.; Wang, S. H.; Yang, S. H. *Chem. Mater.* **1999**, *11*, 3365.

(11) Ding, T.; Zhang, J. R.; Long, S.; Zhu, J. J. *Microelectron. Eng.* **2003**, *66*, 46.

(12) Bakueva, L.; Musikhin, S.; Sargent, E. H.; Ruda, H. E.; Shik, A. In *Handbook of Organic–Inorganic Hybrid Materials and Nanocomposites*; Nalwa, H. S., Ed.; American Scientist: New Haven, CT, 2003.

(13) Han, M.; Gao, X.; Su, J. Z.; Nie, S. *Nat. Biotechnol.* **2001**, *19*, 631.

(14) Lim, L. T.; Kim, S.; Nakayama, A.; Stott, N. E.; Bawendi, M. G.; Frangioni, J. V. *Mol. Imaging* **1998**, *2*, 50.

(15) Bakueva, L.; Musikhin, S.; Hines, M. A.; Chang, T.-W. F.; Tzolov, M.; Scholes, G. D.; Sargent, E. H. *Appl. Phys. Lett.* **2003**, *82*, 2895.

(16) Wundke, K.; Auxier, J.; Schülzgen, A.; Peyghambarian, N.; Borelli, N. F. *Appl. Phys. Lett.* **1999**, *75*, 3060.

(17) Sukhovatkin, V.; Musikhin, S.; Gorelikov, I.; Cauchi, S.; Bakueva, L.; Kumacheva, E.; Sargent, E. H. *Optics Lett.*, in press.

(18) Patel, A. A.; Wu, F.; Zhang, J. Z.; Torres-Martinez, C. L.; Mehra, R. K.; Yang, Yi; Risbud, S. H. *J. Phys. Chem. B* **2000**, *104*, 11598.

(19) Kim, D.; Teratani, N.; Nishimura, H.; Nakayama, M. *Int. J. Mod. Phys. B* **2001**, *15*, 3829.

(20) Hines, M. A.; Scholes, G. D. *Adv. Mater.* **2003**, *15*, 1844;

water-based one-step synthesis, simplicity, use of nontoxic solvents, and low reaction temperatures, stability of photoluminescence properties, and the possibility of NC size tuning (without yield-reducing size-selective precipitation). We showed that these NCs have stable photoluminescence in the near-IR spectral range (1000–1400 nm) when embedded in polymer films or dissolved in aqueous solutions of biopolymers. Moreover, the width of the emission peak was somewhat narrower than that for the PbS NCs obtained by organometallic methods.<sup>20</sup>

Herein, we report a detailed study of the aqueous synthesis of PbS nanoparticles. We examined in detail the effect of a very delicate balance in the concentration ratios of thiol-based stabilizers on the optical properties of NCs. We also investigated kinetics of nucleation and growth and stability of PbS nanoparticles synthesized in aqueous solutions.

### Experimental Section

**Materials.** 1-Thioglycerol (TGL, 95%), dithioglycerol (DTG, 95%), lead(II) acetate trihydrate (99.99%), sodium sulfide nonahydrate (99.99%), and triethylamine were purchased from Sigma-Aldrich and used as received. The water used in all experiments was deionized to a resistivity of 18.2 M $\Omega$ ·cm.

**Synthesis of Semiconductor Nanocrystals.** We carried out synthesis of PbS NCs stabilized with three kinds of capping agents: TGL, DTG, and a mixture of TGL and DTG. When TGL was used as the sole stabilizer, 15 mL of an aqueous solution containing 0.25 mmol of lead(II) acetate and various amounts of TGL was adjusted to pH = 11.2 by adding triethylamine. Then, a 0.1 M solution of sodium sulfide was quickly (<1 s) injected to the system upon vigorous stirring (~1200 rpm). The solution instantly turned from transparent to dark-brown, indicating the formation of PbS nanoparticles. Stirring continued for 5 min.

When DTG was used as the sole stabilizer, the process was similar to that described above but the total amount of DTG used was introduced into the solution in two steps. First, 0.10 mmol of DTG was added with a syringe prior to the addition of triethylamine to prevent the formation of Pb(OH)<sub>2</sub> in a basic solution; then, the remaining DTG was introduced into the system upon vigorous stirring.

In the synthesis of PbS nanoparticles stabilized with TGL and DTG, 15 mL of aqueous solution containing 0.25 mmol of lead(II) acetate trihydrate and 1.5 mmol of TGL was adjusted to pH = 11.2 by the addition of triethylamine. Then, DTG in amounts from 0.11 to 0.96 mmol was injected into the solution. Then, a 0.1 M solution of sodium sulfide was quickly introduced into the system, accompanied by vigorous stirring. The color of the solution instantly or within 10 h (depending on the DTG/Pb molar ratio) changed to dark-brown.

All PbS NCs were produced at room temperature and, unless specified, were not subjected to any postsynthesis, manipulation, or processing. The NCs were stored in an ice bath in the dark for ca. 1 h before their properties were tested, except those that were used in the study of growth kinetics. In the latter case, the NC solutions were stored in the dark at room temperature.

**Nanoparticle Characterization.** Vis–near-IR absorption spectra of PbS NCs were recorded at room temperature using a Cary 500 UV/vis/near-IR spectrophotometer. Fluorescence spectra were measured with a PTI spectrometer with liquid nitrogen cooled Ge detector. Absolute measurements of photoluminescence were carried out in an integrating sphere with excitation provided using an 831 nm semiconductor laser. Transmission electron microscopy (TEM) experiments were performed on a JEOL-2010-FEG microscope operated at 200 kV. The samples were prepared by placing a droplet of diluted NC solution onto a thin carbon-coated copper grid, waiting for ca. 1 min, and then gently wicking away the excess liquid.

Photoluminescence quantum efficiency (PLQE) was determined using a spectralon-coated integrating sphere with a 10 cm inner diameter and two equatorial ports. A liquid waveguide

(Photon Technology International) with transmission in the spectral range from 350 to 2000 nm led from the exit port of the sphere to a grating spectrometer coupled with a liquid nitrogen cooled Ge detector. A two-position sample holder allowed direct or indirect illumination of the sample. The 831 nm excitation laser beam was directed into the sphere through a 2 mm entrance port at near-normal incidence with respect to the cuvette containing the sample. The sample was positioned such that when directly illuminated, any surface reflections were directed onto the sphere wall. The detection system was calibrated by observing the spectral response from a precalibrated tungsten–halogen lamp. The measurements were carried out 2–3 h after NC synthesis was complete.

The experimental procedure and analysis for the absolute determination of photoluminescence quantum efficiency are described elsewhere,<sup>22</sup> wherein spectral measurements of the excitation light and the photoluminescence are performed in three different configurations. These measurements ultimately characterize the absorption of the sample at the pump wavelength, and the resulting photoluminescence independent of the emitted light's spatial distribution.

### Results and Discussion

#### Synthesis of Thiol-Capped PbS Nanocrystals.

When TGL was used as a sole stabilizer, the resulting NCs rapidly increased in size, and ultimately aggregated within 5 h, leading to unstable photoluminescence. Apart from serving as a capping agent, TGL could form strong complexes with lead ions, e.g., polynuclear complexes Pb<sub>3</sub>(RS)<sub>5</sub><sup>+</sup>, Pb<sub>2</sub>RS<sup>3-</sup>, and Pb(RS)<sub>4</sub><sup>2-</sup> or mononuclear species PbRS<sup>+</sup>, Pb(RS)<sub>2</sub>, and Pb(RS)<sub>3</sub><sup>-</sup>, where R is CH<sub>2</sub>(OH)CH<sub>2</sub>(OH)CH<sub>2</sub>–.<sup>23</sup> The formation of all these polynuclear complexes or mononuclear species can account for the rapid aggregation of NCs formed in solution.

When DTG was used as a sole capping agent and the samples were stored at room temperature, the NCs were stable to aggregation for the time period from 2 to 5 weeks (depending on the concentration of lead and sulfur precursors). We found that PbS NCs were formed when the DTG/Pb molar ratio was from 1.70 to 3.83. When an insufficient amount of DTG was used (that is, DTG/Pb < 1.70), a yellow precipitate formed in solution upon addition of DTG (prior to introduction of S<sup>2-</sup>). The precipitate did not disappear with further addition of triethylamine and/or the second part of DTG. For DTG/Pb > 1.70, a yellow precipitate disappeared with addition of DTG. An excess of DTG (DTG/Pb > 3.83) made Pb–DTG bonding so strong that upon subsequent addition of S<sup>2-</sup> ions they did not reach lead ions in the Pb–DTG complex; as a result, no NCs were formed in solution.

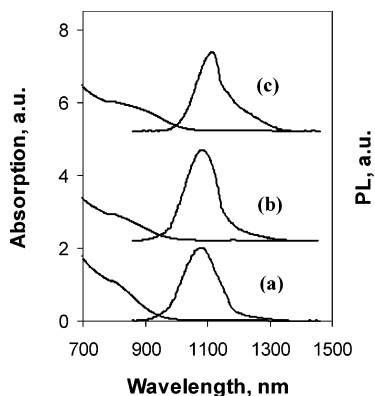
Figure 1 shows absorption and photoluminescence, PL, spectra of PbS NCs capped with a sole DTG stabilizer at DTG/Pb mole ratios in the range of 1.7 < DTG/Pb < 3.83. The absorption shoulder and PL peak (in the range from 900 to 1200 nm) are vastly blue-shifted compared with bulk PbS (band gap energy for bulk-phase PbS is 0.41 eV;  $\lambda_{\text{max}} = 3020$  nm), which was evidence of the strong influence of quantum confinement. The variation in DTG/Pb mole ratio from 2.12 to 2.98 led to a small red shift in absorption and PL spectra of NCs, which indicated that their size slightly increased.

We explored the effect of stabilization of NCs with a mixture of TGL and DTG on NC size tuning, stability, and optical properties. We set the molar ratio TGL/Pb to 6/1 and varied the concentration of DTG in solution. We found that PbS nanoparticles were formed when the DTG/

(22) Tzolov, M.; Brutting, W.; Petrovka-Koch, V.; Gmeiner, J.; Schwoerer, M. *Synth. Mater.* **2001**, *122*, 55.

(23) Milica, T. N.; Mirjana, I. C.; Vesna, V.; Olga, I. M. *J. Phys. Chem.* **1990**, *94*, 6390.

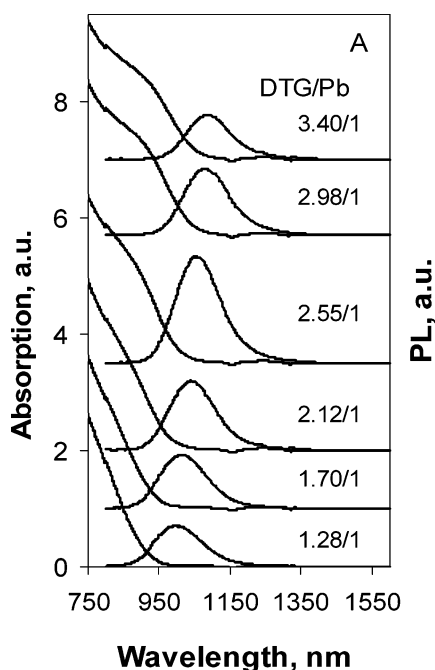
(21) Bakueva, L.; Gorelikov, I.; Musikhin, S.; Zhao, X.; Sargent, E. H.; Kumacheva, E. *Adv. Mater.* **2004**, *16*, 926.



**Figure 1.** Room temperature absorption and PL spectra of freshly prepared PbS NCs capped with DTG. DTG/Pb molar ratio: (a) 2.12/1; (b) 2.55/1; (c) 2.98/1.

Pb molar ratio was from 0.43 to 3.83 (corresponding to a TGL/DTG ratio from 1.57 to 13.95, respectively). The resulting nanoparticles were stable to aggregation under room temperature for 2–3 months (except the series synthesized at DTG/Pb = 0.85). The most stable NCs were obtained at DTG/Pb molar ratios from 1.70 to 2.55.

The concentration of DTG also influenced the optical properties of PbS NCs. In Figure 2A both the absorption shoulder and PL peak of the nanocrystals red-shifted with an increase of the DTG/Pb ratio, which pointed to the increase in size of nanoparticles. This effect is further stressed in Figure 2B: with increasing DTG/Pb molar ratio the wavelength of PL emission shifted from 996 to 1090 nm. We explain this effect as follows. Since at elevated values of pH sulfur atoms are deprotonated producing  $\text{DTG}^{2-}$ ,  $\text{Pb}^{2+}$  ions form complexes with DTG:  $\text{PbDTG}$ ,  $[\text{Pb}(\text{DTG})_2]^{2-}$ , and  $[\text{Pb}(\text{DTG})_3]^{4-}$ . The concentration of each complex depends on the content of DTG in the solution; e.g., an increase in DTG concentration results in an increase in the concentration of  $[\text{Pb}(\text{DTG})_3]^{4-}$  and a decrease in the concentrations of  $\text{PbDTG}$  and  $[\text{Pb}(\text{DTG})_2]^{2-}$ .



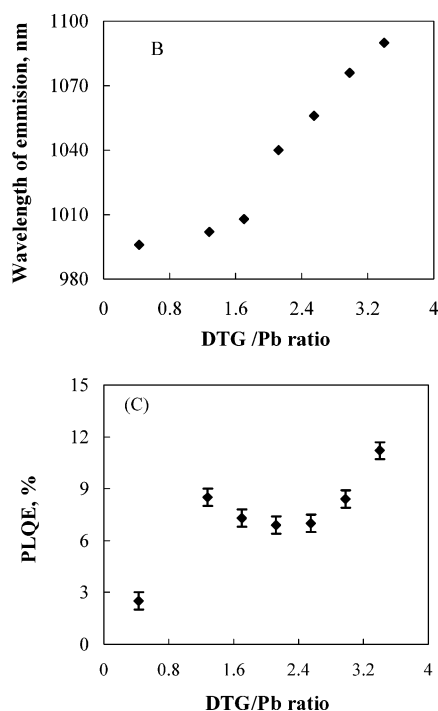
Upon addition of  $\text{S}^{2-}$  ions  $\text{PbDTG}$  and  $[\text{Pb}(\text{DTG})_2]^{2-}$  participate in the nucleation of NCs. By contrast, in the case of  $[\text{Pb}(\text{DTG})_3]^{4-}$ , lead does not react readily with  $\text{S}^{2-}$  ions since its six orbitals participate in bond formation with ligands. In addition, sterical hindrance to NC nucleation is higher in the presence of three ligands than in case of  $\text{PbDTG}$  and  $[\text{Pb}(\text{DTG})_2]^{2-}$ . Thus,  $\text{PbDTG}$  and  $[\text{Pb}(\text{DTG})_2]^{2-}$  contribute to NC nucleation, whereas  $[\text{Pb}(\text{DTG})_3]^{4-}$  serves only as a feeding material. Thus, at higher DTG concentration (favoring the formation of  $[\text{Pb}(\text{DTG})_3]^{4-}$ ) a smaller number of PbS nuclei is formed and the nanoparticle size increases.

Figure 2C shows the variation in photoluminescence quantum efficiency (PLQE) of PbS NCs synthesized at different DTG/Pb ratios. Nanoparticles had a high room-temperature quantum efficiency varying from ca. 7 to 10%, except the series prepared at the smallest DTG/Pb ratio of 0.43/1 for which PLQE was ca. 2%. The PLQE of PbS NCs was stable for at least several weeks when the NC solutions were stored in an ice bath after each measurement.

Typical TEM images of PbS quantum dots synthesized at a DTG/Pb molar ratio of 2.55/1 are shown in Figure 3. The nanoparticles were relatively monodisperse (with the average NC size of  $4 \pm 1$  nm) and well-separated by well-defined gaps. The estimation of NC size on the basis of X-ray diffraction (XRD) analysis gave a similar size.<sup>21</sup>

Comparison of optical properties of PbS NCs stabilized with DTG (Figure 1) and with a TGL/DTG mixture (Figure 2A,B) showed that the use of TGL as a co-stabilizer had relatively little effect on the optical properties of the PbS nanoparticles. TGL played the role of controlling the kinetics of the NCs formation and growth. The formation of NCs slowed to 2 h when the molar ratio TGL/Pb exceeded  $(15 \pm 5)/1$  (for molar ratio DTG/Pb of 2.55/1).

We demonstrated high reproducibility of the synthesis of PbS NCs stabilized with the TGL/DTG mixture by measuring absorption spectra of several exemplary batches of nanocrystals prepared under the same conditions.



**Figure 2.** (A) Absorption and PL spectra of PbS NCs in aqueous solution. The DTG/Pb molar ratio is indicated in the figure. (B) PL peak position as a function of DTG/Pb molar ratio. (C) Room-temperature photoluminescence quantum efficiency of PbS NCs as a function of DTG/Pb molar ratio. All samples were prepared with a mixed stabilizer (TGL/Pb = 6/1).

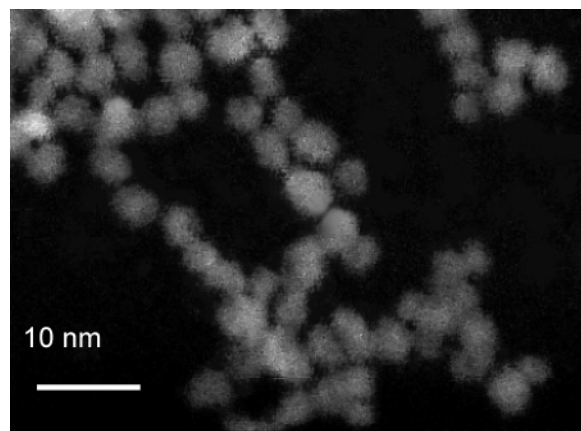


**Figure 3.** Typical dark field TEM image of water-soluble PbS NCs. Molar ratio TGL/DTG/Pb/S = 6/2.55/1/0.5. The sample was dialyzed against deionized water for 24 h.

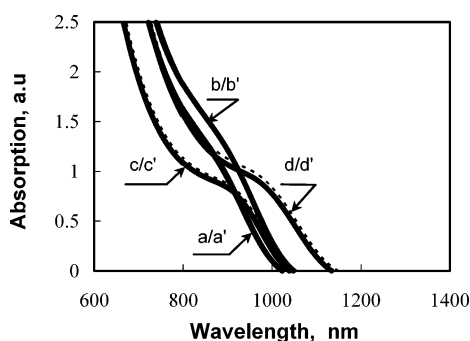


**Figure 4.** Vis-near-IR absorption spectra of freshly prepared PbS NCs. Molar ratio TGL/DTG/Pb/S: 6/0.43/1/0.5 (a/a'); 6/2.12/1/0.5 (b/b'); 6/2.98/1/0.5 (c/c'); 6/3.40/1/0.5 (d/d').

Identical spectra were measured for PbS nanoparticles prepared under the same conditions, especially in systems a and a' (molar ratio TGL/DTG/Pb of 6/0.43/1) and b and b' (TGL/DTG/Pb ratio of 6/2.12/1) (Figure 4).

Typically, the concentration of PbS nanoparticles produced was ca. 3.2 mg/mL. We attempted to scale-up the synthesis of PbS NCs and further optimize the synthetic procedure. Nanoparticles were synthesized at molar ratio TGL/DTG/Pb of 4.8/2.38/1 at increased concentration of NCs of ca. 8.0 mg/mL (and in some reactions up to 20 mg/mL), that is, 2.5–6.0 times as high as in the procedures described above. This synthesis was highly reproducible, and the nanoparticles were stable to aggregation under storage at room temperature for at least 2 months. Figure 5 shows absorption and PL spectra of these nanocrystals. For photoluminescence of the freshly prepared NCs, the full width at half-maximum (fwhm) typically varied from ca. 70 to 100 nm, which are, to the best of our knowledge, the best results reported in the literature for PbS NCs. The room-temperature quantum efficiency was 7.2%, which was in the PLQE range shown in Figure 2C.

The kinetics of growth of PbS nanoparticles was investigated for the samples stored in the dark at room temperature.<sup>24</sup> Figure 6 shows absorption spectra of PbS quantum dots stabilized at molar ratio TGL/DTG/Pb of 6/2.55/1 as a function of time. The absorption shoulder of PbS nanoparticles and the absorption edge red-shifted with time, indicating growth of PbS NCs. Photoluminescence of these NCs showed a similar trend: the PL peak shifted from ca. 950 to 1400 nm and the fwhm increased.

(24) We note that kinetics of the growth of PbS NCs stored in an ice bath is reported in ref 21.

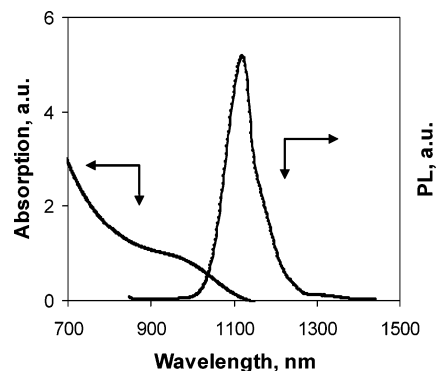


**Figure 5.** Absorption onset and PL peak for PbS NCs capped with a mixed stabilizer in aqueous solution (TGL/DTG/Pb/S = 4.8/2.38/1/0.5; the concentration of NCs in solution is ca. 8.0 mg/mL). The fwhm of the corresponding quantum dots is as narrow as ca. 70 nm.

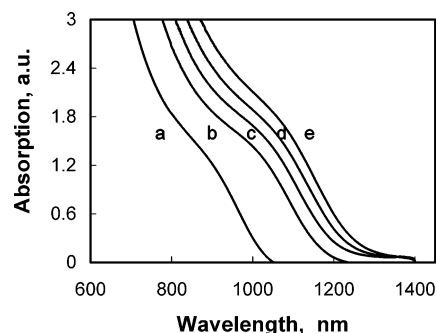


**Figure 6.** Time evolution of vis-IR spectra of PbS NCs stored at room temperature in the dark: (a) freshly prepared NCs; (b) 7 days; (c) 10 days; (d) 14 days; (e) 20 days. The TGL/DTG/Pb molar ratio is 6/2.55/1.

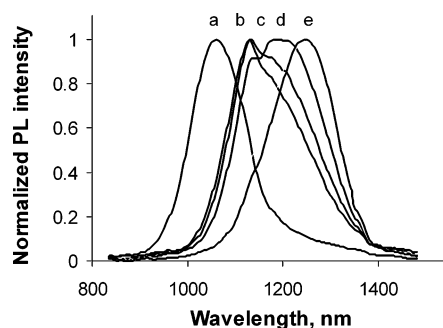


**Figure 7.** Time evolution of photoluminescence of PbS NCs stored at 37 °C in the dark: (a) freshly prepared NCs and after storage for (b) 3, (c) 5, (d) 8, and (e) 15 h. The TGL/DTG/Pb molar ratio is 6/2.55/1.

Nanoparticle size increased due to the Ostwald ripening process: large particles grew at the expense of the smaller ones. We noticed that PbS NCs aggregated in ca. 30–40 days when they were periodically exposed to air during absorption and PL measurements. However, they were stable to aggregation for at least 2–3 months under room temperature when sealed properly immediately after their preparation. Photochemical oxidation of the surface of nanocrystals accounted for the accelerated aggregation and precipitation of the thiol-capped PbS nanoparticles.<sup>3f</sup> Under irradiation the thiol ligands converted into disulfides, which resulted in precipitation of nanocrystals, if no free thiol ligands were available in solution.<sup>25</sup>

(25) We note that an aqueous solution of DTG and triethylamine (in the absence of NPs) was also not stable when exposed to air.

With an eye to applications in fluorescent biolabeling, we measured the evolution in time of the photoluminescence intensity of PbS NCs following their storage at 37 °C. Figure 7 shows the time evolution of PL spectra of the NCs stabilized with a TGL/DTG mixture. After 3 h storage, the shorter wavelength PL maximum measured for the freshly prepared NCs red-shifted and a second PL peak emerged. The two luminescence peaks evolved differently in time: the shorter wavelength peak reduced and ultimately disappeared after 15 h storage. Overall, the PL maximum shifted from 1080 to 1250 nm. We attribute the emergence of two PL peaks to the presence of different fractions of nanoparticles, with the redistribution of peak intensities resulting from Ostwald ripening.

### Conclusions

In summary, we synthesized thiol-capped PbS nanocrystals with stable photoluminescence in the near-IR

spectral range and high-photoluminescence quantum yield. We scaled-up and optimized the synthetic procedure to obtain NCs with a fwhm as narrow as  $85 \pm 15$  nm. Thiol-capped water-soluble PbS NCs stabilized with a mixture of TGL/DTG showed a high stability to aggregation when stored under room temperature in the dark, while individual nanoparticles grew in size. The combination of the narrow fwhm of the PL peak, reasonably good room-temperature quantum efficiency, and good stability makes these NCs a promising material in optical devices, telecommunications, and fluorescent biolabeling.

**Acknowledgment.** The authors acknowledge financial support of NSERC Canada through the Accelerator and Canada Research Chair Program. X.Z. thanks K.C.Wong Education Foundation (Hong Kong) and Guangdong Natural Science Foundation (Grant No. 010525).

LA048730Y